RECURSIVE DIP FILTERS

Jon F. Claerbout and Dave Hale

So-called "pie-slice" filters offer considerable control over the filter response in k/ω dip space. While recursive filters are not controlled as readily, they do meet the same general needs as pie-slice filters and offer the advantages of (1) causality, (2) time- and space-variability, and (3) simple and economic recursive implementation.

Theory

Let P denote raw data and Q denote filtered data. When seismic data are severely band-limited (or quasi-monochromatic), dip filtering can be achieved with spatial frequency filters.

High dip reject:

$$Q = \frac{k_0^2}{k_0^2 + k^2} P \tag{1}$$

Low dip reject:

$$Q = \frac{k^2}{k_0^2 + k^2} P \tag{2}$$

These filters are easily applied in the space domain by interpreting k^2 as a tridiagonal matrix with (-1,2,-1) on the diagonal and k_0^2 as a constant times the identity matrix. One then solves the resulting set of simultaneous equations for Q.

Admitting that seismic data have a bandwidth greater than zero, we are led to consider improved dip filters.

High dip reject:

$$Q_1 = \frac{\frac{k_0^2}{\omega_0}}{\frac{k_0^2}{\omega_0} + \frac{k^2}{-i\omega}} P \tag{3}$$

To understand this filter we need to look in the (ω,k)-plane and draw contours of constant k^2/ω; i.e., $\omega = \alpha k^2$. Such contours, examples of which are shown in figure 1, are curves of constant attenuation and constant phase shift. Inspecting equation (3), we conclude that there is no phase shift in the flat pass zone, but that there is time differentiation in the attenuating zone.

Low dip reject:

$$Q_2 = \frac{\frac{k^2}{-i\omega}}{\frac{k_0^2}{\omega_0} + \frac{k^2}{-i\omega}} P \tag{4}$$

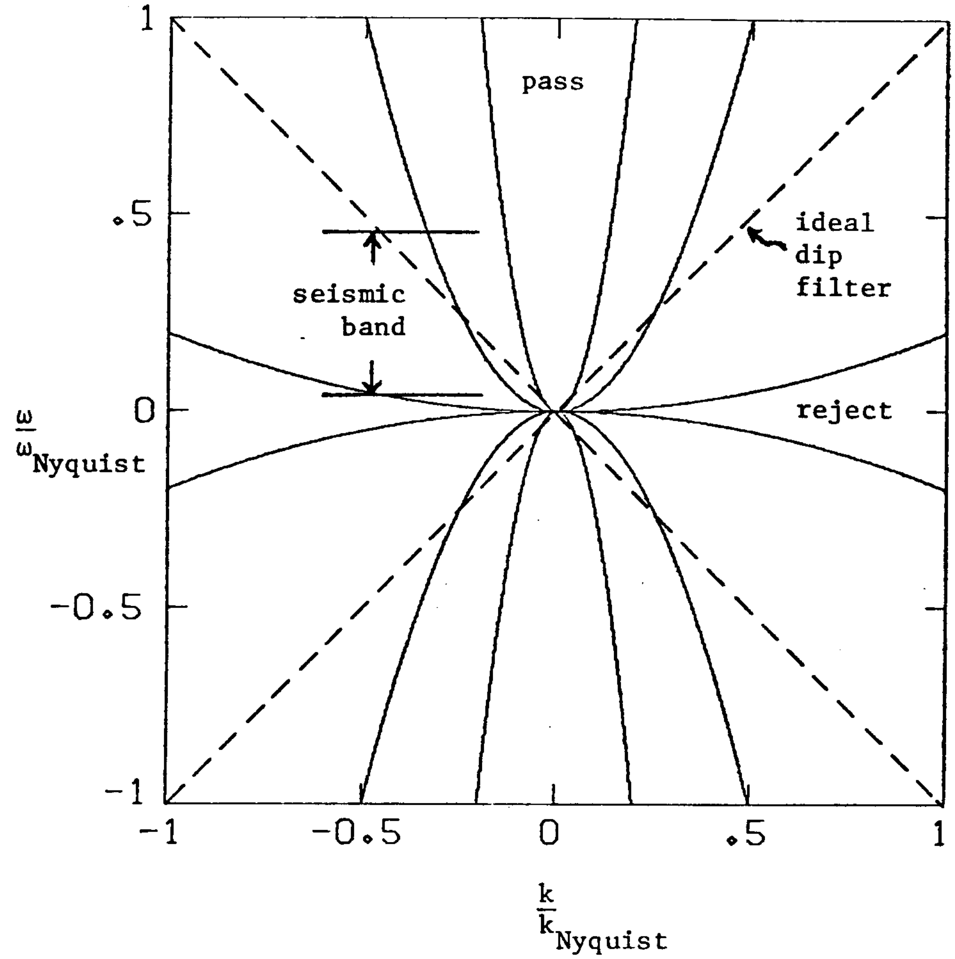

FIG. 1. Constant attenuation contours for the filter of equation (3). Over the seismic frequency band these parabolas may be satisfactory approximations to the dashed straight line.

The filters of equations (3) and (4) behave in opposite ways. (In fact, $Q_1 + Q_2 = P$.) Figure 1 still applies in the case of equation (4), but pass and reject zones are interchanged; and we see temporal integration occur in the reject zone.

An important point is that the filters of equations (3) and (4) are either causal or anticausal, by our choice. To clarify this we multiply the numerator and denominator of (4) by $(-i\omega)$ and apply Muir's rules for impedance functions (see SEP-16, p. 143).

$$Q_2 = \frac{k^2}{-i\omega \frac{k_0^2}{\omega_0} + k^2} P \tag{5}$$

Implementation

Causality permits the implementation of these filters by a straightforward application of the techniques of time domain wave extrapolation as described by Claerbout (1976). Basically, $-i\omega$ is replaced by its Z-transform representation $2(1-Z)/(1+Z)$, and k^2 is replaced by the above-mentioned tridiagonal matrix. Then Q and P are interpreted as vector Z-transforms (i.e., the coefficient of each power of Z is a vector). Clearing out all the fractions and identifying on both sides the coefficient of each power of Z leads to the desired recursive relations. The filters are easily made time- and space-variant by allowing the cutoff parameter, k_0^2/ω_0, to vary with time and space.

Application

Clearly, dip filters may be useful whenever we can discriminate between desired and undesired events on the basis of dip. Now consider the following example. Weak fault diffractions carry velocity information, but they may often be invisible in the presence of stronger horizontal reflections. Dip filtering could be used to attenuate the flat events relative to the more steeply dipping pieces of diffractions. For data recorded at late times and at short offsets, such diffractions could be the only way to measure velocity. This situation applies, for instance, to COCORP data.

In testing the performance of the dip filters of equations (3) and (4), we applied these filters to a window of real data taken from a constant offset section. The data window is shown in figure 2a. Figures 2b and 2c show the results of applying the dip filters of equations (3) and (4), respectively, to this data window. The filtered data of figure 2b illustrate the spatially "mixed" appearance due to rejecting all but the flattest events. But we could see these flat events in the raw data window. The filtered window of figure 2c is more interesting. With the strong horizontal events attenuated, weaker diffraction patterns are more visible, a particularly good example being the diffraction in the upper, left-hand corner of figure 2c which is virtually invisible in the raw data of figure 2a.

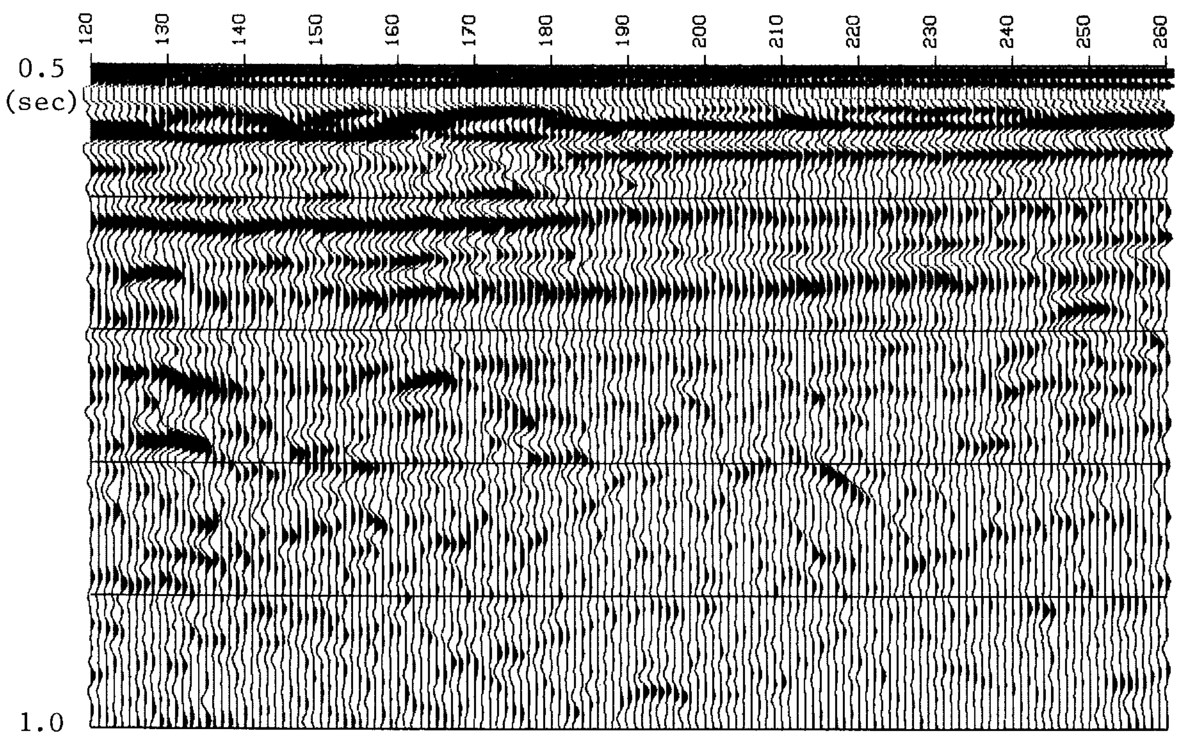

FIG. 2a. The input data window. The strong, horizontal event at 0.5 sec is the water-bottom reflection.

Unanswered Questions

While experience with these filters has shown the parabolic approximation to the straight line to be adequate for many real data examples, one interesting, unanswered question is how to extend the frequency band over which the filters behave like ideal dip filters. Another question is how causal dip filters should be ***defined***. In time series analysis a causal filter is one for which the impulse response vanishes where $t < 0$. In wave propagation we have two-dimensional filters in (x,t)-space or (x,z)-space. Perhaps it should not be the half-space $t < 0$ in the (x,z,t)-volume where the filter vanishes, but the space $t - (x^2 + z^2)^{\frac{1}{2}} < 0$, which is outside a hyperbola in (x,t)-space or a semicircle in (x,z)-space.

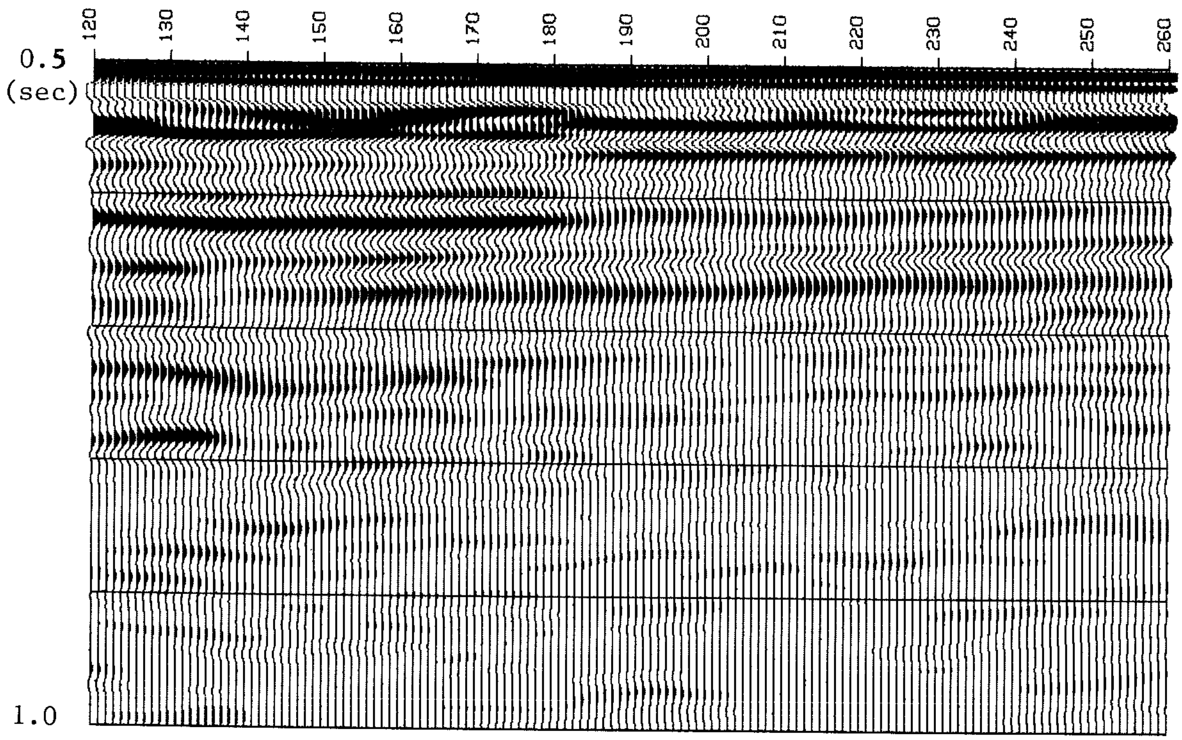

FIG. 2b. The result of applying the high-dip-reject filter of equation (3) to the data window of figure 2a.

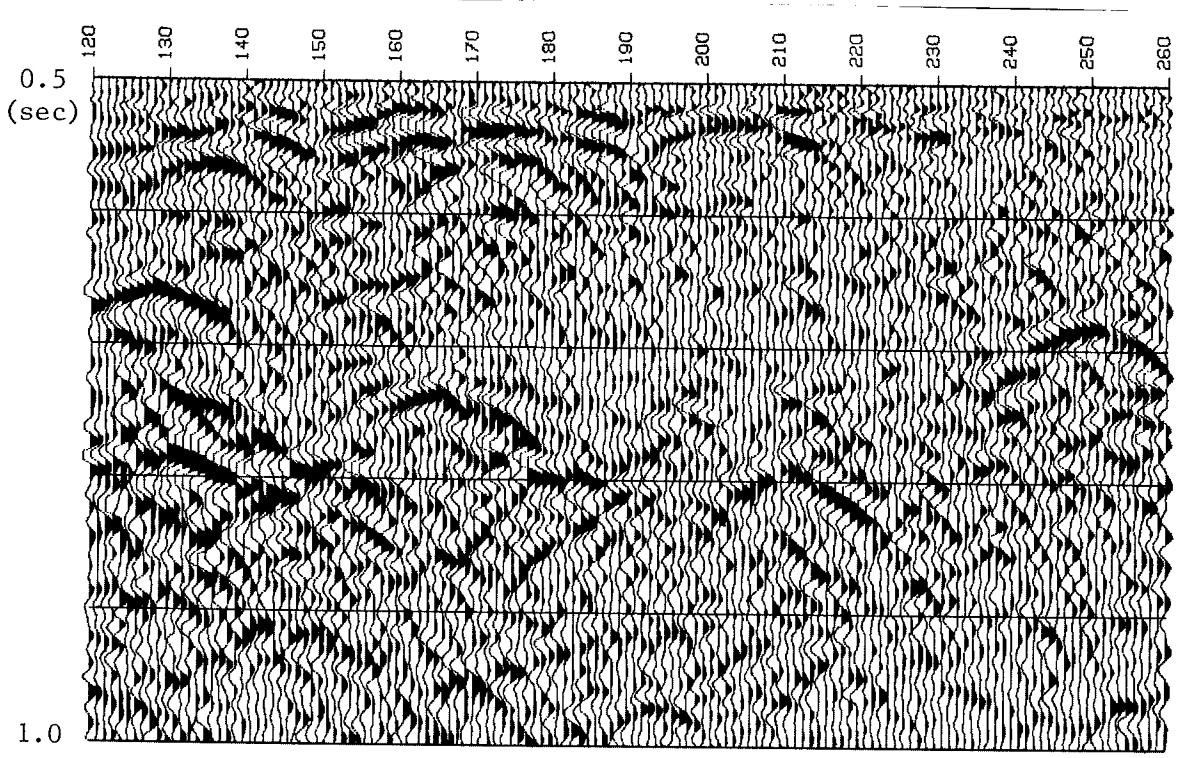

FIG. 2c. The result of applying the low-dip-reject filter of equation (4) to the data window of figure 2a. The weak diffraction patterns are more visible after the flatter events are attenuated.

ACKNOWLEDGMENT

Thanks go to Gulf Research & Development Co. for providing the Gulf of Mexico data shown in this paper.

REFERENCES

Claerbout, Jon F., 1976, Fundamentals of geophysical data processing: New York, McGraw-Hill.

Claerbout, Jon F., 1979, Impedance, reflectance, and transference functions: SEP 16, p. 141-154.